論 文

大 韓 造 船 學 會 誌
第26卷 第1號 1989年 3月
Journal of the Society of
Naval Architects of Korea
Vol. 26, No. 1, March 1989

A Simplified Finite Element Method for the Ultimate Strength Analysis of Plates with Initial Imperfections

by

Jeom K. Paik* and Chang Y. Kim**

초기결함을 가진 판의 최종강도해석을 위한 간이 유한요소법

백 점 기*, 김 창 렬**

Abstract

In this study, an attempt for formulating a new and simplified rectangular finite element having only four corner nodal points is made to analyze the elastic-plastic large deformation behaviour up to the ultimate limit state of plates with initial imperfections. The present finite element contains the geometric nonlinearity caused by both in-plane and out-of-plane large deformation because for very thin plates the influence of the former may not be negligible. Treatment of expanded plastic zone in the plate thickness direction of the element is simplified based upon the concept of plastic node method so that the elastic-plastic stiffness matrix of the element is derived by the simple matrix operation without performing complicated numerical integration. Thus, a considerable saving of the computational efforts is expected.

A computer program is also completed based on the present formulation and numerical calculation for some examples is performed so as to verify the accuracy and validity of the program.

요 약

본 논문에서는 초기부정을 가진 판이 최종강도에 도달하기까지 나타내는 탄소성대변형 거동을 해석하기 위하여 새로운 간이 유한요소법을 개발한다. 본 논문에서 개발하는 유한요소는 4개의 절점만을 가진 4각형 plane-shell요소로서 면외 뿐만아니라 면내의 대변형거동에 의한 기하학적 비선형성의 효과도 고려한다. 또한, 요소의 소성거동에 대한 취급은 소성절점법을 적용하여 판두께방향의 소성영역의 확산을 일일히 고려하는 대신에 판두께방향의 중앙부에 생성되는 소성절점에 집약시켜 나타내는 방법으로 단순화하며, 그 결과, 요소의 탄소성 강성행렬은 판두께방향의 수치적분을 수행할 필요없이 간단한 행렬연산만으로 얻어지기때문에 기존의 유한요소법에 비해 상당한 수치계산 시간의 절약이 예상된다.

본 논문에서 정식화한 해석이론을 바탕으로 컴퓨터 프로그램을 개발하고, 해석예를 통하여 기존의 유한요소법등에 의한 해석결과와 비교하여 본 논문에서 정식화한 해석이론 및 컴퓨터 프로그램의 정도와 유용성을 확인한다.

Manuscript received: September 29, 1988, revised manuscript received: January 24, 1989.

* Member, Dept. of Naval Architecture, Pusan National University (Formerly, ShipResearch Statiou, Korea Institute of Machinery & Metals)

** Member, Dept. of Naval Architecture, Pusan National University

1. Introduction

Plate structures such as ship structures are basically composed of plate elements. As the external load increases, these plate elements show geometric nonlinearity associated with large deformation and material nonlinearity with plasticity until they reach the ultimate limit state. Also, heating processes such as welding and cutting, etc. result in the existence of initial imperfections like initial deflection and residual stress which seriously affect the ultimate strength of plates.

In order to make more reliable design and safety assessment of plate structures, it is essential to have a knowledge for the elastic-plastic large deformation behaviour up to the ultimate limit state of plate elements with initial imperfections.

Finite element method is one of the most powerful approach to analyze nonlinear behaviours of structures but in usual requires enourmous computational efforts which are generally caused by a large number of unknowns and also complicated numerical integration, especially for obtaining the elastic-plastic stiffness matrix of the element.

From the above points of view, this paper describes a formulation of a new and simplified rectangular finite element in an attempt to efficiently analyze the elastic-plastic large deformation behaviour up to the ultimate limit state of plates with initial imperfections.

The novel characteristics of the present finite element are summarized as follows:

1) It is a rectangualr, plane-shell element which has only four corner nodal points having five degrees of freedom in each nodal point.
2) It includes the geometric nonlinear effect due to both in-plane and out-of-plane large deformation of the element because for thin plates widely used in plate structures the influence of the former should be included in a number of cases [1].
3) The expanded yielding zone in the plate thickness direction of the element is condensed into plastic nodes inserted in the nodal point based upon the concept of plastic node method proposed by Ueda et al.[2,3] so that the elastic-plastic stiffness matrix of the element can be calculated by the simple matrix operation without performing complicated numerical integration if once the elastic stiffness matrix is obtained.
4) Above treatments will give a considerable saving of the computational efforts producing the sufficient accuracy.

2. Formulation of the Present Finite Element

2.1. Nodal Force and Displacement Vector of the Element

The combined in-plane and out-of-plane deformation behaviour of a rectangular plate element may be expressed by the nodal force vector $\{R\}$ and displacement vector $\{U\}$ having five degrees of freedom at each corner nodal point which is constructed in the mid-thickness shown in Fig. 1 as

$$\{R\}=\{R_{x1}\ R_{y1}\ R_{z1}\ M_{x1}\ M_{y1}\ R_{x2}\ R_{y2}\ R_{z2}\ M_{x2}\ M_{y2}\ R_{x3}\ R_{y3}\ R_{z3}\ M_{x3}\ M_{y3}\ R_{x4}\ R_{y4}\ R_{z4}\ M_{x4}\ M_{y4}\}^T \quad (1.a)$$

$$\{U\}=\{u_1\ v_1\ w_1\ \theta_{x1}\ \theta_{y1}\ u_2\ v_2\ w_2\ \theta_{x2}\ \theta_{y2}\ u_3\ v_3\ w_3\ \theta_{x3}\ \theta_{y3}\ u_4\ v_4\ w_4\ \theta_{x4}\ \theta_{y4}\}^T \quad (1.b)$$

$$\theta_x=-\partial w/\partial y,\quad \theta_y=\partial w/\partial x$$

where R_x, R_y and R_z are axial forces in the x, y and z direction and M_x and M_y are out-of-plane bending moments with regard to x and y direction, respectively. Also, u, v and w are displacements in the x, y and z direction and θ_x and θ_y are rotations with regard

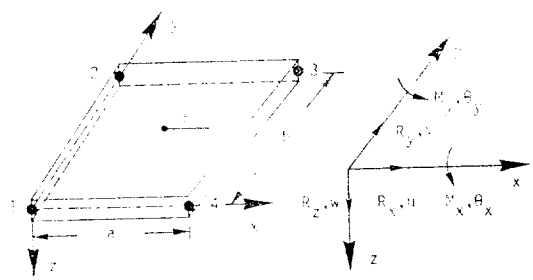

Fig. 1. The local coordinate of a rectangular plate element and its nodal forces and displacements

to x and y direction, respectively and superscript T denotes an transporse of the vector or matrix.

2.2. Relationship Between Strains and Displacements

The strain-displacement relation taking large deformation effects for out-of-plane as well as in-plane of the element into consideration is given in the cartesian coordinate system shown in Fig. 1 as[4]

$$\varepsilon_x=\frac{\partial u}{\partial x}-z\frac{\partial^2 w}{\partial x^2}+\frac{1}{2}\left\{\left(\frac{\partial u}{\partial x}\right)^2+\left(\frac{\partial v}{\partial x}\right)^2\right\}+\frac{1}{2}\left(\frac{\partial w}{\partial x}\right)^2$$

$$\varepsilon_y=\frac{\partial v}{\partial y}-z\frac{\partial^2 w}{\partial y^2}+\frac{1}{2}\left\{\left(\frac{\partial u}{\partial y}\right)^2+\left(\frac{\partial v}{\partial y}\right)^2\right\}+\frac{1}{2}\left(\frac{\partial w}{\partial y}\right)^2$$

$$\gamma_{xy}=\left(\frac{\partial u}{\partial y}+\frac{\partial v}{\partial x}\right)-2z\frac{\partial^2 w}{\partial x\partial y}+\left\{\left(\frac{\partial u}{\partial x}\right)\left(\frac{\partial u}{\partial y}\right)+\left(\frac{\partial v}{\partial x}\ \frac{\partial v}{\partial y}\right)\right\}+\left(\frac{\partial w}{\partial x}\right)\left(\frac{\partial w}{\partial y}\right) \tag{2}$$

where $\varepsilon_x, \varepsilon_y$ and γ_{xy} denote the generalized strain components for a plane stress state and the first term at the right hand side of each equation indicate the small in-plane strain components due to in-plane deformation and likewise the second term denotes the small out-of-plane strain components due to out-of-plane deformation. Also, the third and fourth term are nonlinear strain components due to large deformation for in-plane and out-of-plane, respectively.

The incremental expression of Eq. (2) is written as

$$\Delta\varepsilon_x=\frac{\partial \Delta u}{\partial x}-z\frac{\partial^2 \Delta w}{\partial x^2}+\left(\frac{\partial u}{\partial x}\right)\left(\frac{\partial \Delta u}{\partial x}\right)+\left(\frac{\partial v}{\partial x}\right)\left(\frac{\partial \Delta v}{\partial x}\right)+\left(\frac{\partial w}{\partial x}\right)\left(\frac{\partial \Delta w}{\partial x}\right)$$
$$+\frac{1}{2}\left\{\left(\frac{\partial \Delta u}{\partial x}\right)^2+\left(\frac{\partial \Delta v}{\partial x}\right)^2\right\}+\frac{1}{2}\left(\frac{\partial \Delta w}{\partial x}\right)^2$$

$$\Delta\varepsilon_y=\frac{\partial \Delta v}{\partial y}-z\frac{\partial^2 \Delta w}{\partial y^2}+\left(\frac{\partial u}{\partial y}\right)\left(\frac{\partial \Delta u}{\partial y}\right)+\left(\frac{\partial v}{\partial y}\right)\left(\frac{\partial \Delta v}{\partial y}\right)+\left(\frac{\partial w}{\partial y}\right)\left(\frac{\partial \Delta w}{\partial y}\right)$$
$$+\frac{1}{2}\left\{\left(\frac{\partial \Delta u}{\partial y}\right)^2+\left(\frac{\partial \Delta v}{\partial y}\right)^2\right\}+\frac{1}{2}\left(\frac{\partial \Delta w}{\partial y}\right)^2$$

$$\Delta\gamma_{xy}=\left(\frac{\partial \Delta u}{\partial y}+\frac{\partial \Delta v}{\partial x}\right)-2z\frac{\partial^2 \Delta w}{\partial x\partial y}+\left(\frac{\partial u}{\partial x}\right)\left(\frac{\partial \Delta u}{\partial y}\right)+\left(\frac{\partial u}{\partial y}\right)\left(\frac{\partial \Delta u}{\partial x}\right)+\left(\frac{\partial v}{\partial x}\right)\left(\frac{\partial \Delta v}{\partial y}\right)+\left(\frac{\partial v}{\partial y}\right)\left(\frac{\partial \Delta v}{\partial x}\right)$$
$$+\left(\frac{\partial w}{\partial x}\right)\left(\frac{\partial \Delta w}{\partial y}\right)+\left(\frac{\partial w}{\partial y}\right)\left(\frac{\partial \Delta w}{\partial x}\right)+\left(\frac{\partial \Delta u}{\partial x}\right)\left(\frac{\partial \Delta u}{\partial y}\right)+\left(\frac{\partial \Delta v}{\partial x}\right)\left(\frac{\partial \Delta u}{\partial y}\right)+\left(\frac{\partial \Delta w}{\partial x}\right)\left(\frac{\partial \Delta w}{\partial y}\right) \tag{3}$$

where prefix Δ denotes the infinitesimal increment of the variable.

For a plane-shell element, since the nodal displacement vector $\{U\}$ can be separated into $\{S\}$ and $\{W\}$ which are defined as the in-plane and out-of-plane component of the vector $\{U\}$, respectively, Eq.(3) is rewritten by the matrix form using the vectors $\{S\}$ and $\{W\}$ as

$$\{\Delta\varepsilon\}=[B_p]\{\Delta S\}-Z[B_b]\{\Delta W\}+[C_p][G_p]\{\Delta S\}$$
$$+[C_b][G_b]\{\Delta W\}+\frac{1}{2}[\Delta C_p][G_p]\{\Delta S\}$$
$$+\frac{1}{2}[\Delta C_b][G_b]\{\Delta W\}$$
$$=[B]\{\Delta U\} \tag{4}$$

where, $\{\Delta\varepsilon\}=\{\Delta\varepsilon_x\ \Delta\varepsilon_y\ \Delta\gamma_{xy}\}^T$

: the increment of strain component

$\{U\}=\{S\,W\}^T$

: the nodal displacement vector

$\{S\}=\{u_1\ v_1\ u_2\ v_2\ u_3\ v_3\ u_4\ v_4\}^T$

: the in-plane component of displacement vector

$\{W\}=\{w_1\ \theta_{x1}\ \theta_{y1}\ w_2\ \theta_{x2}\ \theta_{y2}\ w_3\ \theta_{x3}\ \theta_{y3}\ w_4\ \theta_{x4}\ \theta_{y4}\}$

: the out-of-plane component of displacement vector

$[B]$: the strain-displacement matrix

$$\begin{Bmatrix}\frac{\partial u}{\partial x}\\ \frac{\partial v}{\partial y}\\ \frac{\partial u}{\partial y}+\frac{\partial v}{\partial x}\end{Bmatrix}=[B_p]\{S\},\quad \begin{Bmatrix}\frac{\partial^2 w}{\partial x^2}\\ \frac{\partial^2 w}{\partial y^2}\\ 2\frac{\partial^2 w}{\partial x\partial y}\end{Bmatrix}=[B_b]\{W\},$$

$$\begin{Bmatrix}\frac{\partial u}{\partial x}\\ \frac{\partial v}{\partial x}\\ \frac{\partial u}{\partial y}\\ \frac{\partial v}{\partial y}\end{Bmatrix}=[G_p]\{S\},\quad \begin{Bmatrix}\frac{\partial w}{\partial x}\\ \frac{\partial w}{\partial y}\end{Bmatrix}=[G_b]\{W\},$$

$$[C_p]=\begin{bmatrix} \frac{\partial u}{\partial x} & \frac{\partial v}{\partial x} & 0 & 0 \\ 0 & 0 & \frac{\partial u}{\partial y} & \frac{\partial v}{\partial y} \\ \frac{\partial u}{\partial y} & \frac{\partial v}{\partial y} & \frac{\partial u}{\partial x} & \frac{\partial v}{\partial x} \end{bmatrix},\quad [C_b]=\begin{bmatrix} \frac{\partial w}{\partial x} & 0 \\ 0 & \frac{\partial w}{\partial y} \\ \frac{\partial w}{\partial y} & \frac{\partial w}{\partial x} \end{bmatrix} \tag{5}$$

2.3. Relationship Between Membrane Stresses and Strains

Membrane stress increment $\{\Delta\sigma\}$ due to strain increment $\{\Delta\varepsilon\}$ is calculated for a plane stress state as

$$\{\Delta\sigma\}=[D]^e\ \{\Delta\varepsilon\}^e \tag{6}$$

where, $\{\Delta\sigma\}=\{\Delta\sigma_x\ \Delta\sigma_y\ \Delta\tau_{xy}\}^T$

: the increment of average membrane stress components for a plane stress state

$$[D]^e=\frac{E}{1-\nu^2}\begin{bmatrix} 1 & \nu & 0 \\ \nu & 1 & 0 \\ 0 & 0 & \frac{1-\nu}{2} \end{bmatrix} \tag{7}$$

: the elastic stress-strain matrix

E : Young's modulus

ν : Poisson's ratio

Also, superscript e in Eq.(6) denotes the elastic range.

2.4. Derivation of the Tangent Elastic Stiffness Matrix in the Local Coordinate

2.4.1. Total Lagrangian Formulation

Considering that the structure under the acting of the nodal force $\{R\}$ which results in the producing of the internal stress $\{\sigma\}$ is in equilibrium, if the structure remains the equilibrium state even after the additional acting of the virtual displacement increment $\delta\{\Delta U\}$ corresponding to the virtual strain increment $\delta\{\Delta\varepsilon\}$ which develops the nodal force $\{\Delta R\}$ and the resultant stress $\{\Delta\sigma\}$, the following equation should be satisfied by the principle of the virtual work[5].

$$\delta\{\Delta U\}^T\{R+\Delta R\}=\int_V\delta\{\Delta\varepsilon\}^T\{\sigma+\Delta\sigma\}\,\mathrm{dVol} \tag{8}$$

where the left side term represents the external work done by the virtual displacement increment and the right side indicates strain energy stored during the action of the virtual strain increment and also $\int_V(\bullet)$ dVol denotes the integrating for the entire volume of the element and prefix δ denotes the virtual.

The virtual strain increment $\delta\{\Delta\varepsilon\}$ is obtained by differentiating Eq. (4) with respect to the increment of the variable as

$$\begin{aligned}\delta\{\Delta\varepsilon\}=&[B_p]\delta\{\Delta S\}-z[B_b]\delta\{\Delta W\}\\&+[C_p+\Delta C_p][G_p]\delta\{\Delta S\}\\&+[C_b+\Delta C_b][G_b]\delta\{\Delta W\}\end{aligned} \tag{9}$$

Substituting Eq.(6) and (9) into Eq.(8) and neglecting the infinitesimal terms having higher order of the increment in comparison with just one order of the increment, the elastic stiffness equation of the element in the local coordinate system is finally expressed as

$$\{L\}+\{\Delta R\}=[K]^e\{\Delta U\} \tag{10}$$

where, $[K]^e$: the tangent elastic stiffness matrix of the element

$\{L\}=\{R\}-\{r\}$

: the unbalance force caused by the discrepancy between the total external force $\{R\}$ and the total internal force $\{r\}$

Also, the total internal force $\{r\}$ in Eq.(10) is calculated as

$$\begin{aligned}\{r\}=&\int_V[B_p]^T\{\sigma\}\,\mathrm{dVol}+\int_V[G_p]^T[C_p]^T\{\sigma\}\,\mathrm{dVol}\\&+\int_V[G_b]^T[C_b]^T\{\sigma\}\,\mathrm{dVol}\end{aligned} \tag{11}$$

where, $\{\sigma\}=\{\sigma_x\ \sigma_y\ \tau_{xy}\}^T$

: :the total average membrane stress components

By the way, the tangent stiffness matrix $[K]^e$ in Eq.(10) may be subdivided into four terms as

$$[K]^e=[K_P]+[K_B]+[K_G]+[K_\sigma] \tag{12}$$

In the right hand side of Eq.(12), the first and the second term represent stiffness matrices related to the in-plane and out-of-plane small deformation, respectively. The third term, so called initial deformation stiffness matrix consists of three terms representing the geometric nonlinear effect associated with in-plane deformation, out-of-plane deformation and their interactions. The fourth term is so called initial stress stiffness matrix which is produced by the existence of initial stress and consists of two terms related to the in-plane and out-of-plane large deformation in which the term to their interactions is not appeared.

Each term mentioned above is obtained in detail as

$$[K_P]=\left[\begin{array}{c|c}[K_1] & 0\\ \hline 0 & 0\end{array}\right],\quad [K_B]=\left[\begin{array}{c|c}0 & 0\\ \hline 0 & [K_2]\end{array}\right],$$

$$[K_G]=\left[\begin{array}{c|c}[K_3] & [K_4]\\ \hline [K_4]^T & [K_5]\end{array}\right],\quad [K_\sigma]=\left[\begin{array}{c|c}[K_6] & 0\\ \hline 0 & [K_7]\end{array}\right] \tag{13.a}$$

where, $[K_1]=\int_V [B_p]^T[D]^e[B_p]\mathrm{dVol}$,

$[K_2]=\int_V [B_b]^T[D]^e[B_b]\cdot z^2\mathrm{dVol}$,

$[K_3]=\int_V [G_p]^T[C_p]^T[D]^e[B_p]\mathrm{dVol}$
$+\int_V [B_p]^T[D]^e[C_p][G_p]\mathrm{dVol}$
$+\int_V [G_p]^T[C_p]^T[D]^e[C_p][G_p]\mathrm{dVol}$,

$[K_4]=\int_V [B_p]^T[D]^e[C_b][G_b]\mathrm{dVol}$
$+\int_V [G_p]^T[C_p]^T[D]^e[C_b][G_b]\mathrm{dVol}$,

$[K_5]=\int_V [G_b]^T[C_b]^T[D]^e[C_b][G_b]\mathrm{dVol}$,

$[K_6]=\int_V [G_p]^T[\sigma_p][G_p]\mathrm{dVol}$,

$[K_7]=\int_V [G_b]^T[\sigma_b][G_b]\mathrm{dVol}$,

$$[\sigma_p]=\begin{bmatrix}\sigma_x & 0 & \tau_{xy} & 0\\ 0 & \sigma_x & 0 & \tau_{xy}\\ \tau_{xy} & 0 & \sigma_y & 0\\ 0 & \tau_{xy} & 0 & \sigma_y\end{bmatrix},$$

$$[\sigma_b]=\begin{bmatrix}\sigma_x & \tau_{xy}\\ \tau_{xy} & \sigma_y\end{bmatrix} \tag{13.b}$$

In calculating Eq. (13), terms including one order of the variable "z" which would become to be zero by completing the integration for the entire volume of the element in the elastic range and even in the elastic-plastic range because the inside of the element except for plastic nodes is considered to be always elastic in this study, were eliminated.

2.4.2. Updated Lagrangian Formulation

The stiffness matrix $[K]^e$ in Eq. (12) was derived under the consideration that the local coordinate of the element is fixed with ragard to the global space one, which results in the possibility of the use of the identical transformaton matrix through every incremental loading steps.

On the other hand, using the concept of updated Lagrangian formulation in which the local coordinate may become to be altered and updated in each deformed state of the element so that the transformation matrix from the local to the global coordinate should be newly set up, the initial deformation stiffness matrix $[K_G]$ in Eq. (12) can be removed because the initial deformation in the beginning of each incremental loading step has become to be eliminated. Thus, the stiffness equation will be written by three terms as

$$[K]^e=[K_p]+[K_B]+[K_\sigma] \tag{14}$$

2.5. Displacement Function

In this study, the bi-linear function for the in-plane displacement of u and v and the polynomial function which is expressed in terms of the twelve parameters for the out-of-plane displacement of w are adopted as [6]

$$\begin{aligned}u&=a_1+a_2x+a_3y+a_4xy\\ v&=b_1+b_2x+b_3y+b_4xy\\ w&=c_1+c_2x+c_3y+c_4x^2+c_5xy+c_6y^2+c_7x^3\\ &\quad+c_8x^2y+c_9xy^2+c_{10}y^3+c_{11}x^3y+c_{12}xy^3\end{aligned} \tag{15}$$

where, $a_1, a_2\cdots c_{12}$ are unknown coefficients which are expressed in terms of nodal displacements $\{U\}$ by the usual manner of the finite element tecnique. Then, substituting Eq. (4) and (15) into Eq. (12) for the total Lagrangian formulation and into Eq. (14) for the updated Lagrangian formulation and also finishing all volume integrations, components of the tangent elastic stiffness matrix $[K]^e$ of the element in the local coordinate will be obtained. Here, since the stiffness matrix $[K]^e$ is nonlinear with regard to the deformation, it should be newly calculated at every incremental loading steps.

2.6. Yielding Condition

In this study, plasticity of the element is checked in the corner nodal points located in the middle plane of the cross-section. Also, the fully plastic condition under combined in-plane and out-of-plane loads through the cross-section of the element is used as a yielding condition. Then, the yielding condition in the i th nodal point, which is expressed in terms of the resultant membrane stress and generalized bending stress components will be given by the nondimensional expression as[3]

$$F_i=n_i^2+|m_i|-1=0 \tag{16}$$

where, $n_i^2=n_{xi}^2-n_{xi}n_{yi}+n_{yi}^2+3n_{xyi}^2$

$m_i^2=m_{xi}^2-m_{xi}\,m_{yi}+m_{yi}^2+3m_{xyi}^2$

$n_{xi}=\sigma_{xi}/\sigma_0$, $n_{yi}=\sigma_{yi}/\sigma_0$, $n_{xyi}=\tau_{xyi}/\sigma_0$

$m_{xi}=2\sigma_{xbi}/3\sigma_0$, $m_{yi}=2\sigma_{ybi}/3\sigma_0$, $m_{xyi}=2\tau_{xybi}/3\sigma_0$

$\{\sigma_i\}=\{\sigma_{xi}\ \sigma_{yi}\ \tau_{xyi}\}^T$

: the nodal membrane stress components

$\{\sigma_{bi}\}=\{\sigma_{xbi}\ \sigma_{ybi}\ \tau_{xybi}\}^T$

: the nodal maximum generalized bending stress components developed in the outer fiber of the cross-section[3]

σ_0 : the yielding stress of the element material

Also, subscript i denotes the i th nodal point.

The resultant membrane and bending stress components used in Eq.(16) can be obtained by the accumulation of the increment of the corresponding components through each loading step. Also, the increment of stress components in the i th nodal point is calculated as

$$\{\Delta\sigma_i\}=[D]^e\{\Delta\varepsilon\}^e=[D]^e[B_i]\{\Delta U\}^e \quad (17.a)$$

$$\{\Delta\sigma_{bi}\}=-t^2/6[D]^e\{\Delta\varepsilon\}^e=-t^2/6[D]^e[B_{bi}]\{\Delta W\}^e \quad (17.b)$$

where, $[B_i]$ and $[B_{bi}]$ which are the functions of the variables of x and y indicate the strain-displacement matrices being substituted the local coordinate for the ith nodal point into x and y of Eq.(4). Also, for the calculation of the bending stress components, only out-of-plane displacement $\{\Delta W\}^e$ is needed because the generalized bending stress is independent of the in-plane displacement $\{\Delta S\}$ as discribed in Eq.(17.b).

Eq.(16) may be sketched as shown in Fig.2 and the curve in the figure is termed as the yielding surface. Thus, if the value of the yielding function at any nodal point is less than zero, which implies that the value of the yielding function is located in the inside of the yielding surface, like in point A of Fig.2, the condition of this nodal point is still elastic, but when it reaches zero with the increasing of the external load, which likewise indicates that the value of the yielding function is just at the yielding surface, like in point B or B' of Fig. 2, the state of that nodal point becomes to be plastic and then the plastic node is inserted at such a nodal point but the inside of the element is considered to be elastic. In reality, however, it is very difficult to secure that the value of the yielding function is just at the yielding surface since the response is nonlinear. Thus, in this study, the smallest magnification factor for the initially prescribed load to make a yielding only one nodal point among all elastic nodes is linearly predicted in advance (see Appendix I). Then, elastic nodes are yielded one by one through the incremental loading step so that the value of the yielding function will be located just or very near in the yielding surface. However, if the value of the yielding function is in the outside of the yielding surface, like in point C of Fig. 2, which represents that the prescribed load increment was too big, the load increment should be corrected and the iteration of the procedure is necessary until the desired accuracy is obtained.

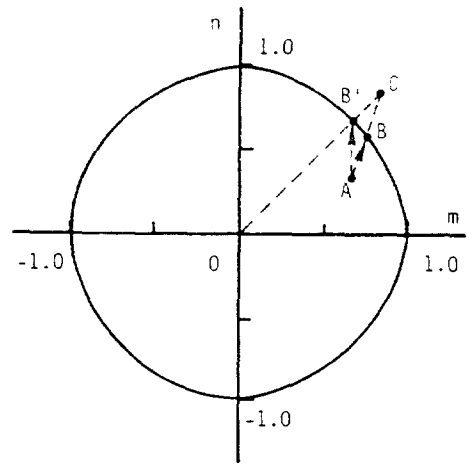

Fig. 2. A diagram of the yielding surface

2.7. Derivation of the Tangent Elastic-Plastic Stiffness Matrix in the Local Coordinate

In this study, the tangent elastic-plastic stiffness matrix of the element in the local coordinate system is derived based upon the concept of plastic node method proposed by Ueda et al.[2, 3].

After attaining the convergence for the unbalance force $\{L\}$ in Eq.(10), e.g. securing the equilibrium state of the structure, the tangent elastic stiffness equation of the element will become as

$$\{\Delta R\}=[K]^e\{\Delta U\}^e \quad (18)$$

where $[K]^e$ is equal to Eq.(12) for the total Lagrangian formulation and to Eq.(14) for the updated Lagrangian formulation and $\{\Delta U\}^e$ is the elastic

component of displacement increment which is identified with the total displacement increment $\{\Delta U\}$ if the element is still in the elastic range. Also, since the nodal force vector is related to only the elastic component of displacement, Eq.(18) should be noted even in the elastic-plastic range.

If the resultant stress components in any nodal points of the element satisfy the plastic condition of Eq.(16), the plastic nodes are inserted and the plastic deformation will be produced. Thus, the total displacement increment $\{\Delta U\}$ is calculated by summing up the elastic and plastic component of displacement increment as

$$\{\Delta U\}=\{\Delta U\}^e+\{\Delta U\}^p \tag{19}$$

where, $\{\Delta U\}^p$ is the plastic component of displacement increment in which superscript p denotes the plastic range.

Under the consideration that yielding function is the plastic potential, the following definition for the plastic component of displacement increment is made after the i th nodal point has bocome to be plastic by using Drucker's normality rule [7].

$$\{\Delta U\}^p=\Delta\lambda_i\{\phi_i\},\quad \{\phi_i\}=\left\{\frac{\partial F_i}{\partial R}\right\} \tag{20}$$

where, $\Delta\lambda_i$ is a positive scalar characterizing the magnitude of the plastic displacement and $\{\phi_i\}$ is the outward normal vector to the yielding surface as shown in Fig.3.

Also, the vector $\{\phi_i\}$ in Eq.(20) can be calculated by using a relation between the resultant stresses and the nodal forces(see Appendix II).

When the resultant stress components at the i th nodal point satisfy the yielding condition, the value of the yielding function will be located at the yielding surface like in point O of Fig. 3.a, in which the normal vector $\{\phi_i\}_O$ will be produced. With the increasing of the external load, since the normal forces at a plastic node move along a tangent direction to the yielding surface, the point O will move to point A located in the outside of the yielding surface and the normal vector $\{\phi_i\}_A$ will be produced. And likewise in the next step, the point A will move to point B which may be more different than point A from the yielding surface, in which the normal vector $\{\phi_i\}_B$ will be produced.

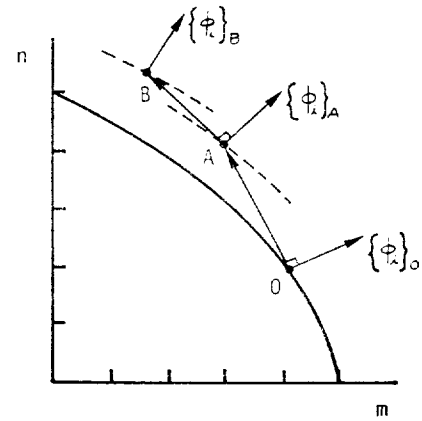

Fig. 3.a The drift of the value of the yielding function

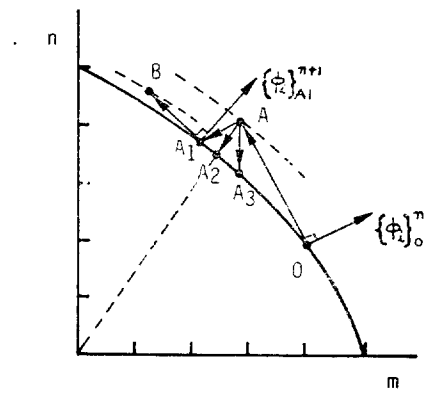

Fig. 3.b A two-step procedure for the convergence of the yielding condition [11]

In this procedure, however, since the value of the yielding function is in the outside of the yielding surface, the normal vector $\{\phi_i\}$ is not real and if the drift from the yielding surface is relatively large, any results in the subsequent procedure are no longer reliable.

Thus, for controlling the drift of the value of the yielding function from the yielding surface, several approaches have been proposed, in which iterative methods [8], one-step force correction methods [9] and five-step procedures [10] are useful.

In this study, however, a new two-step procedure

[11] is proposed and applied: As mentioned in the previous section, the elastic nodes of the structure are yielded one by one through the incremental loading step so that the value of the yielding function will be located just or very near in the yielding surface. Then, as shown in Fig. 3.b, if the value of the yielding function at the i th nodal point is considered to be located in point O in the n th loading step, we get the normal vector $\{\phi_i\}_O^n$. Thus, with the increasing of the external load, the value of the yielding function will move to point A along the tangent vector $\overrightarrow{OA}$. Here, if the drift of point A from the yielding surface exceeds the acceptable tolerance, the point A is made a correction to point A_1 or A_2 or A_3 by using the linearly determined corection factor, which is also obtained in the same manner of the calculation of the load magnification factor indicated in Appendix II. Then, for example, if point A is considered to be returned to point A_1, the nodal forces will produce the normal vector $\{\phi_i\}_{A1}^{n+1}$ and the tangent vector $\overrightarrow{A_1B}$ for the $(n+1)$ th loading step. This approach may produce some errors but is very simple and gives sufficient accuracy for the practical purpose[11].

Thus, if m numbers of the nodal point in an element are under the plastic condition, the plastic component of displacement increment $\{\Delta U\}^p$ is then calculated by superposing Eq.(20) as

$$\{\Delta U\}^p=\sum_{i=1}^{m}\Delta\lambda_i\{\phi_i\},\quad m=1,2,3,4 \tag{21}$$

Substituting Eq.(19) and (21) into Eq.(18), the stiffness equation becomes as

$$\{\Delta R\}=[K]^e(\{\Delta U\}-\sum_{i=1}^{m}\Delta\lambda_i\{\phi_i\}) \tag{22}$$

Neglecting the strain hardening effect, e.g. considering the elastic-fully plastic material, the following equation should be satisfied at every plastic nodes as far as the loading process continues.

$$\Delta F_i=\{\phi_i\}^T\{\Delta R\}=0 \tag{23}$$

Substituting Eq.(22) into Eq.(23), the unknown parameter $\Delta\lambda$ is obtained as

$$\{\Delta\lambda\}=[\Phi]^T[K]^e([\Phi]^T[K]^e[\Phi])^{-1}\{\Delta U\} \tag{24}$$

where, $[\Phi]=[\{\phi_1\}\{\phi_2\}\cdots\{\phi_m\}]^T$

$\{\Delta\lambda\}=\{\Delta\lambda_1\ \Delta\lambda_2\cdots\Delta\lambda_m\}^T$

Also, superscript (-1) denotes an inverse of the matrix.

Thus, the tangent stiffness equation of the element in the elastic-plastic range is gained by substituting Eq.(24) into Eq.(22) again as

$$\{\Delta R\}=[[K]^e-[K]^e[\Phi][\Phi]^T[K]^e([\Phi]^T[K]^e[\Phi])^{-1}$$
$$\{\Delta U\}=[K]^p\{\Delta U\} \tag{25}$$

where $[K]^p$ is the elastic-plastic stiffness matrix of the element and $[K]^e$ is the elastic stiffness matrix derived in the section 2.4.

It is clear from Eq.(25) that the elastic-plastic stiffness matrix $[K]^p$ can be calculated by the simple matrix operation without performing numerical integration over the volume of the element if once the elastic stiffness matrix$[K]^e$ is obtained.

In the calculation of Eq.(25), the loading state at every plastic nodes should be checked and when the unloading is detected, i.e. if $\Delta\lambda_i<0$, the plastic node should be treated as an elastic.

2.8. Transformation Matrix to the Global Coordinate

In general, an exact formulation of the transformation matrix for the rectangular plate element is difficult to define so that the approximate assuming that the element is in a plane containg at least three nodal points of the element is made in this study.

Thus, the transformation matrix $[T]$ from the local to the global coordinate is written in the cartesian coordinate system shown in Fig. 4 as [6]

$$[T]=\begin{pmatrix}[\alpha] & & & \\ & [\alpha] & & \\ & & [\alpha] & \\ & & & [\alpha]\end{pmatrix} \tag{26.a}$$

$$[\alpha]=\begin{pmatrix}\alpha_{x'x} & \alpha_{x'y} & \alpha_{x'z} & 0 & 0\\ \alpha_{y'x} & \alpha_{y'y} & \alpha_{y'z} & 0 & 0\\ \alpha_{z'x} & \alpha_{z'y} & \alpha_{z'z} & 0 & 0\\ 0 & 0 & 0 & \alpha_{y'y} & \alpha_{y'x}\\ 0 & 0 & 0 & \alpha_{x'y} & \alpha_{x'x}\end{pmatrix} \tag{26.b}$$

where the blank space in Eq.(26.a) indicates zero term and $\alpha_{x'x}$, etc. are direction cosines between x' axis in the deformed state and x axis in the original one as shown in Fig. 4.

By applying Eq.(26), the element stiffness matrix in the local coordinate will be tranformed to the

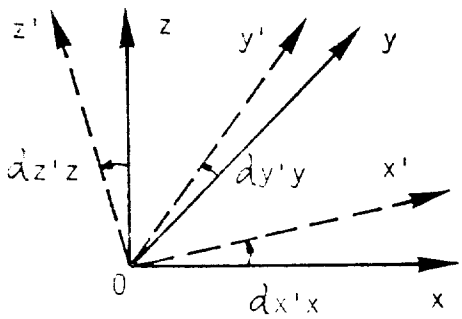

Fig. 4. Local and global coordinates

global coordinate as

$$[K]_g=[T]^T[K]_l[T] \tag{27}$$

where $[K]_l$ and $[K]_g$ are the element stiffness matrices in the local and global coordinate, respectively.

Thus, all element stiffness matrices in the global coordinate are then assembled by the usual manner to get the whole structure stiffness matrix and by solving the stiffness equation under the specified incremental load and/or displacement, the structural response will be obtained.

3. Numerical Examples and Discussions

3.1. Solution strategy

Based upon the present finite element, a computer program was completed in this study. The computer program applies updated Lagrangian formulation for deriving the elastic stiffness matrix, skyline method [12] for solving the stiffness equation and Newton-Rapson iteration procedure [13] for eliminating the unbalance force.

In this study, the initial deflection existed in the plate element is treated to be initial deformation at the nodal points so that the coordinate of the nodal points is updated from the flat plate state in the first loading step, in which the resultant stresses due to the initial deformation are not taken into account.

Also, the residual stress is considered to be initial membrane stress of the element which is directly concerned with the initial stress stiffness matrix $[K_\sigma]$ in Eq.(12) or (14) and the yielding function in Eq. (16): As shown in Fig. 5, when the welding process is provided along the longitudinal edges of the plate, an actual distribution of the residual stress is produced by the solid line characterizing the self-equilibrium between the tensile and compressive residual stress and in general the magnitude of the tensile residual stress developed in the heat affected zone reaches the yielding stress, σ_0 in the case of the mild steel. Here, an idealized residual stress distribution indicated by the dotted line is introduced and then a relation between the tensile and compressive residual stress is formulated by the self-equilibrium condition as

$$\frac{\sigma_{rx}}{\sigma_0}=\frac{2b_t}{b-2b_t}$$

where σ_{rx} denotes the magnitude of the longitudinal compressive residual stress developed in the middle of the plate and $2b_t$ represents the total breadth of the strip acted by the tensile residual stress(see Fig. 5). Then, for the present numerical analysis, the idealized distribution and magnitude of the residual stress is inputed as nodal membrane stresses in the first loading step in which the mesh size depends on the breadth of the strip, b_t so that the influence of the residual stress is involved for deriving the initial stress stiffness matrix $[K_\sigma]$ in Eq. (12) or (14) and checking the yielding condition of Eq. (16) but it should be excluded for the calculation of the total internal force $\{r\}$ in Eq. (11). And even though the transverse residual stress which is produced when the welding process is provided in the transverse edges of the plate, or combined the longitudinal and transverse residual stress is existed, the same procedure

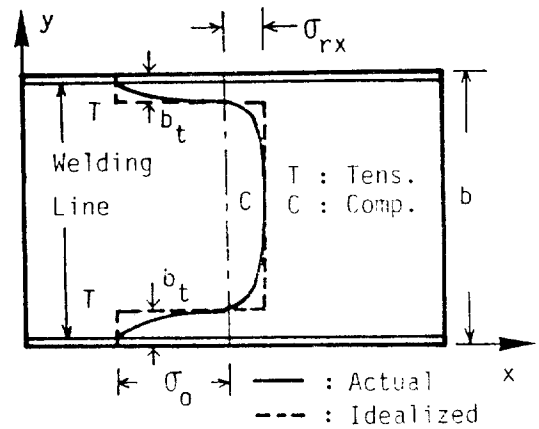

Fig. 5. A typical distribution of the welding residual stress

is applied.

Within each incremental loading step, iteration procedure to secure the equilibrium of the structure is performed until the desired accuracy is gained. The convergence check is carried out by comparing the relative change of the norm of the selected displacement vector as

$$\frac{\|U_i - U_{i-1}\|}{\|U_{i-1}\|} < \epsilon$$

where $\|U_{i-1}\|$ and $\|U_i\|$ are the norms of the selected displacement vectors in the $(i-1)$th and i th iteration, respectively and ϵ is the termination criterion which is set by 0.01 in this study.

3.2. Accuracy Assessment and Application of the Present Method

(1) Elastic-Plastic Large Deformation Analysis of a Square Flat Plate Subjected to Uniform Edge Displacement

As shown in Fig. 6, a simply supported square plate subjected to uniform edge displacement is analyzed. The unloaded edges can be moved in the in-plane direction but remain straight. Only a quarter of the plate is modelled by 5×5 mesh due to the symmetry. The plate has very small initial deflection of $w_0/t=0.01$ of which shape is considered to be sinuisoidal curve where w_0 is the amplitude of the initial deflection at center.

Fig. 6.a and 6.b show the load-central deflection curve for the typical thin and thick plates, respectively and also the yielding history of the plate is presented in the same figure. The present results are compared to the conventional finite element solution by Ueda et al. [14]. They applied 10×10 mesh model for a quarter of the plate using the triangular plane-shell element with three corner nodal points and subdivided the plate thickness into 20 layers so that they took the effect of the expanded yielding zone in the plate thickness direction into consideration.

For the thin plate shown in Fig. 6.a, after the elastic buckling takes place in which the theoretical elastic buckling strength σ_{cr}/σ_0 is 0.4, the plastic nodes are started in the corner of the unloaded edges where the large membrane stresses are developed due to the condition of straight boundary and expanded

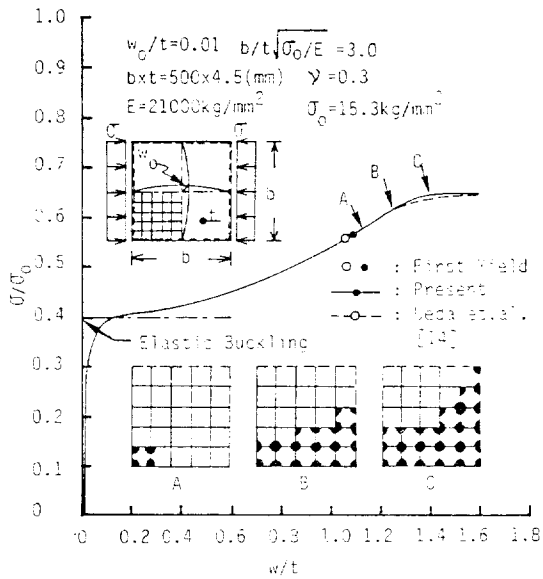

Fig. 6.a The load-central deflection curve of a simply supported square plate subjected to uniform edge displacement(unloaded edges remain straight)

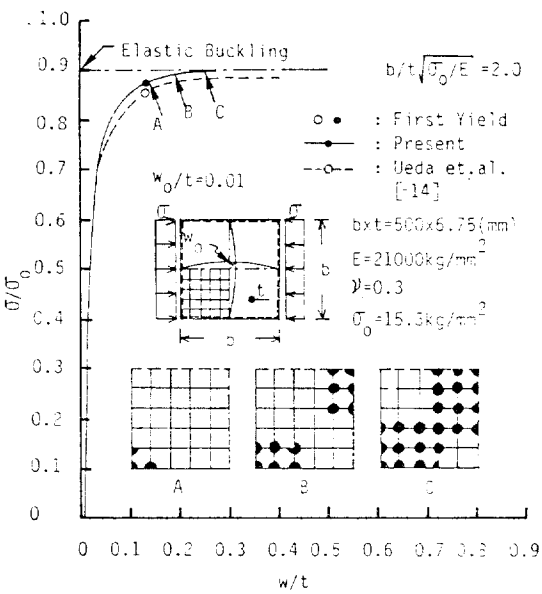

Fig. 6.b The load-central deflection curve of a simply supported square plate subjected to uniform edge displacement(unloaded edges remain straight)

to the center with the increasing of the bending stresses due to the large deflection. On the other hand, the thick plate shown in Fig. 6.b shows the

elastic-plastic buckling phenomenon in which the teoretical elastic buckling strength, $\sigma_{cr}/\sigma_0=0.9$ and since the membrane stresses are dominant everywhere of the plate the plastic nodes are started in the corner of the unloaded edges and also at the center.

Comparing the present and conventional finite element solution, the present method slightly overestimates the ultimate strength of the plate. This is due that the mesh size of the present modelling is somewhat coarse and the fully plastic condition through the cross-section is used as a yielding condition in this study. However, the accuracy is sufficient for the practical purpose and it is clear that the present method gives the reliable buckling and ultimate strength of the plate. For this example, the computing time was about 5 minitues by PRIME 6350 computer.

(2) Influence of the Magnitude of the Initial Deflection on the Ultimate Strength of a Square Plate Subjected to Uniform Edge Displacement

The elastic-plastic large deformation behaviour of a square plate subjected to uniform edge displacement is also analyzed varying the magnitude of the initial deflection whose shape is also considered to be sinuisoidal curve as shown in Fig. 7. The boundary of the plate is simply supported and the in-plane displacements of the unloaded edges are unrestrained so that little membrane stresses in the transverse

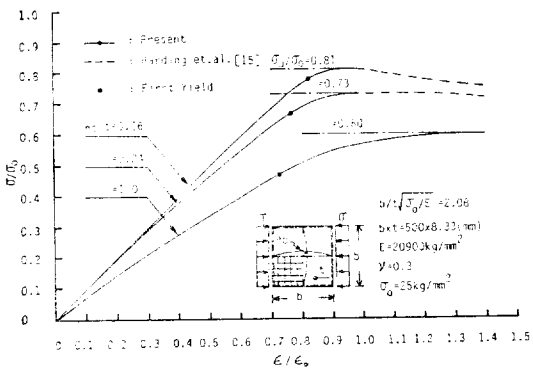

Fig. 7.a The load-shortening curve of a simply supported square plate subjected to uniform edge displacement (unloaded edges are unrestrained)

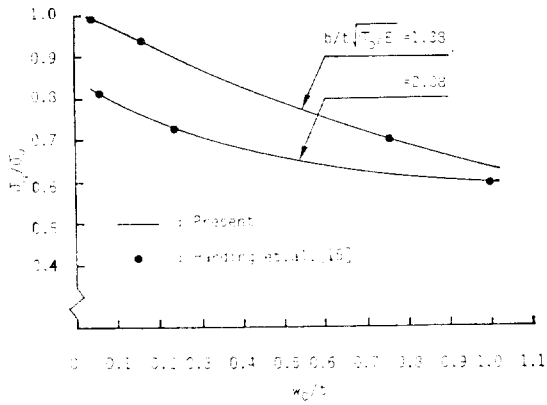

Fig. 7.b The load-shortening curve of a simply supported plate subjected to uniform edge displacement (unloaded edges are unrestrained)

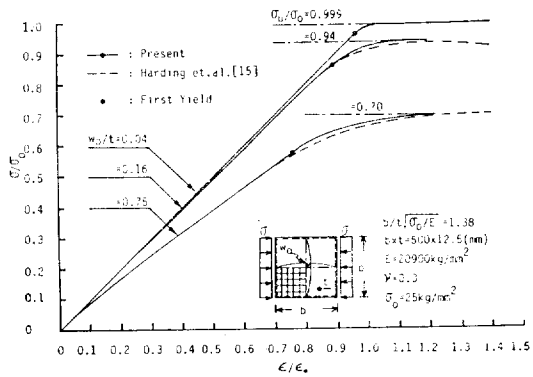

Fig. 7.c Influence of the magnitude of the initial deflection on the ultimate strength of a simply supported square plate subjected to uniform edge displacement (unloaded edges are unrestrained)

direction may occur. 5×5 mesh modelling for a quarter of the plate is also adopted.

Fig. 7.a and 7.b represent the load-shortening curve, where ϵ_0 presented in the figure is the fully plastic strain, $\epsilon_0=\sigma_0/E$, for two plates with divers initial deflections and Fig. 7.c shows the influence of the magnitude of the initial deflection on the ultimate strength of the plate.

Fig. 7 indicates that with the increasing of the initial deflection, the in-plane stiffness of the plate decreases from the beginning and a large amount of the ultimate strength is reduced. The present results are also compared to the conventional finite element

solution by Harding et al. [15]. It is also clear from Fig. 7 that the present method gives the accurate elastic-plastic large deformation response up to the ultimate strength of the plate with the initial deflection. For this example, the computing time was about 3~5 minitues by PRIME 6350 computer.

(3) Influence of the Residual Stress on the Ultimate Strength of a Square Plate Subjected to Uniform Edge Displacement

The influence of the existence of residual stress mainly due to welding on the ultimate strength is also investigated varying the magnitude of the residual stress. The shape of the initial deflection, mesh size, the boundary and loading condition are identified with the case of (1) but the magnitude of the initial deflection is set as $w_0/t=0.05$ and the plate has the longitudinal residual stress.

Fig. 8.a and 8.b represent the load-central deflection curve for two plates with divers residual stresses and Fig. 8.c shows the influence of the residual stress on the ultimate strength of the plate. Fig. 8 indicates that with the increasing of the residual stress, both buckling and ultimate strength are reduced by amount of about the magnitude of the compressive residual stress. The present results are also compared to the approximate semi-analytical solution by Little [16] which used Von Mises condition as a yielding condition expressed in terms

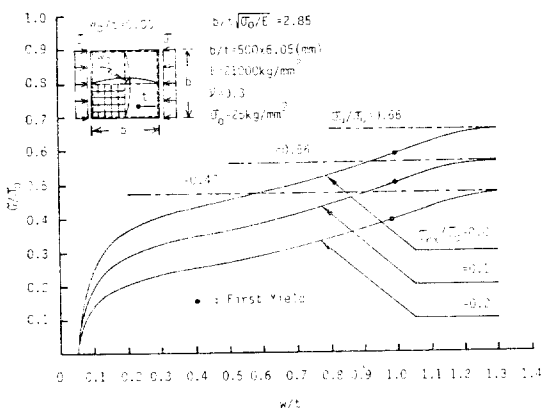

Fig. 8.a The load-central deflection curve of a simply supported square plate subjected to uniform edge displacement(unloaded edges remain straight)

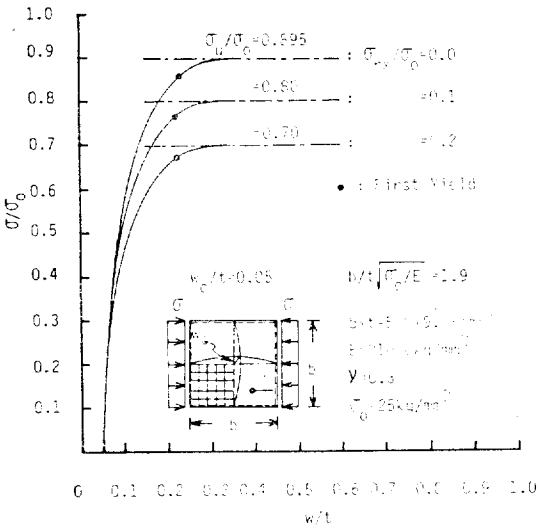

Fig. 8.b The load-central deflection curve of a simply supported square plate subjected to uniform edge displacement(unloaded edges remain straight)

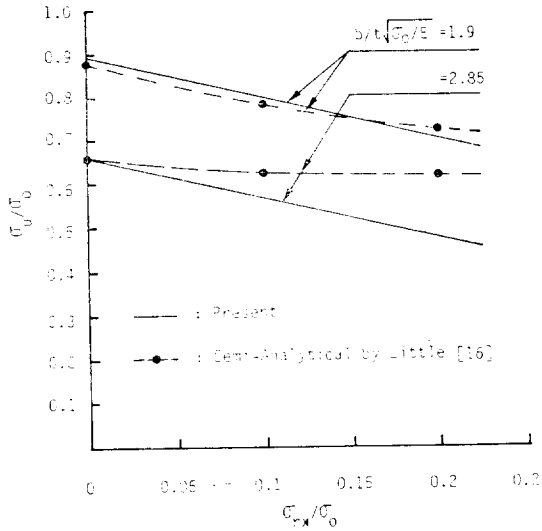

Fig. 8.c Influence of the magnitude of the residual stress on the ultimate strength of a simply supported square plate subjected to uniform edge displacement(unloaded edges remain straight)

of only membrane stress components. Thus, for thick plates shown in Fig. 8.b, in which the membrane stresses are dominant the present results are in good agreement with Little's solution but for thin plates shown in Fig. 8.a, since both the membrane and

bending stresses are dominant, Little's approach overestimates the ultimate strength. For this example, the computing time was also about 3~5 minitues by PRIME 6350 computer.

4. Conclusion

Through some numerical examples presented in this study, it is possible to make a conclusion as

(1) The present method gives sufficient accuracy for the problems of the elastic-plastic large deformation analysis up to the ultimate limit state of plates with initial imperfections.

(2) The computing time is reasonable since for the case of 5×5 mesh modelling, about 3~5 minitues by PRIME 6350 computer were required.

Acknowledgement

The present study was conducted at Ship Research Station, Korea Institute of Machinery & Metals when the first author was working there. The authors wish to express their sincere gratitudes to Dr. Ho S. Lee who is a head of Ship Structure Division, SRS, KIMM for his helpful support.

References

[1] H.G. Allen and H.H. Al-Qarra, "Geometrically Nonlinear Analysis Structural Membranes", *Computers & Structures*, Vol. 25, No. 6, 1987.

[2] Y. Ueda and T. Yao, "The Plastic Node Method: A New Method of Plastic Analysis", *J. of Computer Methods in Applied Mechanics and Engineers*, Vol. 34, No. 1-3, 1982.

[3] Y. Ueda, T. Yao and M. Fujikubo, "Generalization of the Plastic Hinge Method", *J. of Society of Naval Architects of Japan*, Vol. 146, 1979 (in Japanese).

[4] A.E.H. Love, "A Treatise on the Mathematical Theory of Elasticity", Dover Publications, New York, 1944.

[5] K. Washizu, "Variational Methods in Elasticity and Plasticity", Pergamon Press, 1968.

[6] O.C. Zienkiewicz, "The Finite Element Method", 3rd Edition, McGraw-Hill, New York, 1977.

[7] D.C. Drucker, "A More Fundamental Approach to Plastic Stress-Strain Relations", *Proceeding of the First U.S. National Congress of Applied Mechanics*, Chicago, Illinois, 1951.

[8] R.K. Wen and F. Farhoomand, "Dynamic Analysis of Inelastic Space Frames", *J. of Engineering Mechanics Division*, ASCE, Vol. 96, No. 5, 1970.

[9] R.O. Krieg and O.B. Krieg, "Accuracies of Numerical Solution Methods for the Elastic-Perfectly Plastic Model", *J. of Pressure Vessel Technique*, ASME, Vol. 94, No. 4, 1977.

[10] J.G. Orbison, W. Mcguire and J.F. Abel, "Yield Surface Applications in Nonlinear Steel Frame Analysis", *J. of Computer Methods in Applied Mechanics and Engineering* Vol. 33, 1982.

[11] J.K. Paik, "A New Two-Step Procedure for the Convergence of Yielding Condition" (in Preparation).

[12] K.J. Bathe and E.L. Wilson,"Numerical Methods in Finite Element Analysis", Prentice-Hall, 1976.

[13] E. Isaacson and H.B. Keller, "Analysis of Numerical Methods", John Willey and Sons, New York, 1966.

[14] Y. Ueda and T. Yao, "The Influence of Complex Initial Deflection Modes on the Behaviour and Ultimate Strength of Rectangular Plates in Compression", *J. of Construction Steel Research*, Vol. 5, 1985.

[15] I.E. Harding, R.E. Hobbs and B.G. Neal, "The Elasto-Plastic Analysis of Imperfect Square Plates Under In-Plane Loading", *Proc. Inst. Civil Engineers*, Part 2, Vol. 63, 1977.

[16] G.H. Little, "The Collapse of Rectangular Steel Plates Under Uniaxial Compression", *The Structural Engineer*, Vol. 58B, No. 3, 1980.

Appendix I. The Load Magnification Factor

Due to the acting of the incremental prescribed load $\{\Delta R\}$ in the nth loading step, if the total and the increment of the resultant stress components are

defined by $\{\sigma\}$, $\{\sigma_b\}$ and $\{\Delta\sigma\}$, $\{\Delta\sigma_b\}$, respectively, the magnitude of the incremental external load in the next loading step which will satisfy the yielding condition in a nodal point is given by $\beta\{\Delta R\}$ where a multiplier β is defined as the positive load magnification factor:

From the yielding condition of Eq.(16), the following wing equation emerges.

$$\begin{aligned}&(n_x+\beta\Delta n_x)^2-(n_x+\beta\Delta n_x)(n_y+\beta\Delta n_y)+(n_y+\beta\Delta n_y)^2\\&+3(n_{xy}+\beta\Delta n_{xy})^2+\{(m_x+\beta\Delta m_x)^2\\&-(m_x+\beta\Delta m_x)(m_y+\beta\Delta m_y)+(m_y+\beta\Delta m_y)^2\\&+3(m_{xy}+\beta\Delta m_{xy})^2\}^{1/2}-1=0\end{aligned}\tag{A.1}$$

Neglecing the infinitesimal terms, Eq.(A.1) becomes as

$$\left(A+\frac{D}{2\sqrt{F}}\right)\beta^2+\left(B+\frac{E}{2\sqrt{F}}\right)\beta+C+\sqrt{F}-1=0\tag{A.2}$$

where, $A=\Delta n_x^2-\Delta n_x\Delta n_y+\Delta n_y^2+3\Delta n_{xy}^2$

$B=(2n_x-n_y)\Delta n_x+(2n_y-n_x)\Delta n_y+6n_{xy}\Delta n_{xy}$

$C=n_x^2-n_xn_y+n_y^2+3n_{xy}^2$

$D=\Delta m_x^2-\Delta m_x\Delta m_y+\Delta m_y^2+3\Delta m_{xy}^2$

$E=(2m_x-m_y)\Delta m_x+(2m_y-m_x)\Delta m_y+6m_{xy}\Delta m_{xy}$

$F=m_x^2-m_xm_y+m_y^2+3m_{xy}^2$

Thus, the positive load magnification factor β is obtained as

$$\beta=\frac{-\alpha_2+\sqrt{\alpha_2^2-4\alpha_1\alpha_3}}{2\alpha_1}\tag{A.3}$$

where, $\alpha_1=A+\frac{D}{2\sqrt{F}}$, $\alpha_2=B+\frac{E}{2\sqrt{F}}$,

$\alpha_3=C+\sqrt{F}-1$

In actual numerical procedure, the smallest value of β which yields only one nodal point acting by the biggest stresses among all the elastic nodes is determined and also since the response is nonlinear, it is recomended that the value of β less than 1.0 is set.

Appendix II. The Outward Normal Vector $\{\phi\}$

Eliminating the unbalance force, the stiffness equation of the element is given by Eq.(10) as

$$\{\Delta R\}=[K]^e\{\Delta U\}^e\tag{A.4}$$

and

$$\{\Delta R_w\}=[K_w]^e\{\Delta W\}\tag{A.5}$$

where subscript w denotes the vetcor or matrix for the out-of-plane component.

Also, the stress-displacement relation in the ith nodal point of the element is written by Eq.(17) as

$$\{\Delta\sigma_i\}=[D]^e[B_i]\{\Delta U\}^e\tag{A.6}$$

$$\{\Delta\sigma_{bi}\}=-t^2/6[D]^e[B_{bi}]\{\Delta W\}^e\tag{A.7}$$

Removing the rigid body motion, Eq.(A.4), (A.5), (A.6) and (A.7) become as

$$\{\Delta R\}=[K^*]^e\{\Delta U^*\}^e\tag{A.8}$$

$$\{\Delta R_w\}=[K_w^*]^e\{\Delta W^*\}^e\tag{A.9}$$

$$\{\Delta\sigma_i\}=[D]^e[B_i^*]\{\Delta U^*\}^e\tag{A.10}$$

$$\{\Delta\sigma_{bi}\}=-t^2/6[D^e][B_{bi}^*]\{\Delta W^*\}^e\tag{A.11}$$

where asterisk indicates reduced degrees of freedom after removing the rigid body motion of the element.

Calculating the nodal displacements $\{\Delta U^*\}^e$ and $\{\Delta W^*\}^e$ being got rid of the rigid body motion from Eq.(A.8) and (A.9) and substituting them into Eq.(A.10) and (A.11), the following relation between the resultant stresses and the nodal forces is obtained.

$$\{\Delta\sigma_i\}=[D]^e[B_i^*]([K^*]^{eT}[K^*]^e)^{-1}[K^*]^{eT}\{\Delta R\}\tag{A.12}$$

$$\{\Delta\sigma_{bi}\}=-t^2/6[D]^e[B_{bi}^*]([K_w^*]^{eT}[K_w^*]^e)^{-1}[K_w^*]^{eT}\{\Delta R_w\}\tag{A.13}$$

Also, the vector $\{\phi_i\}$ reads

$$\{\phi_i\}=\sigma_0^2\left(\left\{\frac{\partial F_i}{\partial\sigma_i}\right\}^T\left\{\frac{\partial\sigma_i}{\partial R}\right\}+\left\{\frac{\partial F_i}{\partial\sigma_{bi}}\right\}^T\left\{\frac{\partial\sigma_{bi}}{\partial R_w}\right\}\right)\tag{A.14}$$

where the multiplying value of σ_0^2 was appeared because the yielding condition of Eq.(16) was expressed by the nondimensional function.

In Eq.(A.14), $\left\{\frac{\partial F_i}{\partial\sigma_i}\right\}$ and $\left\{\frac{\partial F_i}{\partial\sigma_{bi}}\right\}$ are calculated by differentiating the yielding function of Eq.(16) with regard to the stress components. Thus,

$$\sigma_0^2\cdot\left\{\frac{\partial F_i}{\partial\sigma_i}\right\}=\{2\sigma_{xi}-\sigma_{yi},\ 2\sigma_{yi}-\sigma_{xi},\ 6\tau_{xyi}\}^T\tag{A.15}$$

$$\sigma_0^2\cdot\left\{\frac{\partial F_i}{\partial\sigma_{bi}}\right\}=\left\{\frac{\sigma_0}{3\sqrt{S}}(2\sigma_{xbi}-\sigma_{ybi}),\ \frac{\sigma_0}{3\sqrt{S}}(2\sigma_{ybi}-\sigma_{xbi}),\ \frac{2\sigma_0}{\sqrt{S}}\tau_{xybi}\right\}^T\tag{A.16}$$

where, $S=\sigma_{xbi}^2-\sigma_{xbi}\ \sigma_{ybi}+\sigma_{ybi}^2+3\tau_{xybi}^2$

Also, $\left\{\frac{\partial\sigma_i}{\partial R}\right\}$ and $\left\{\frac{\partial\sigma_{bi}}{\partial R_w}\right\}$ are given from Eq.(A.

12) and (A.13) as

$$\left\{\frac{\partial \sigma_i}{\partial R}\right\}=[D]^e\ [B_*^i]\ ([K^*]^{eT}\ [K^*]^e)^{-1}\ [K^*]^{eT} \tag{A.17}$$

$$\left\{\frac{\partial \sigma_{bi}}{\partial R_w}\right\}=-t^2/6[D]^e\ [B_{bi}^*]\ ([K_w^*]^{eT}\ [K_w^*]^e)^{-1}\ [K_w^*]^{eT} \tag{A.18}$$

Then, the normal vector $\{\phi_i\}$ in the ith nodal point is calculated by substituing Eq. (A.15), (A. 16), (A.17) and (A.18) into Eq. (A.14).